# Intra-Data Center 120Gbaud/DP-16QAM Self-Homodyne Coherent Links with Simplified Coherent DSP

Rui Zhang<sup>1,2</sup>, You-Wei Chen<sup>2</sup>, Konstantin Kuzmin<sup>2</sup>, and Winston I. Way<sup>2</sup>

(1) School of Electrical and Computer Engineering, Georgia Institute of Technology, Atlanta, GA 30332, USA
 (2) NeoPhotonics, 3081 Zanker Road, San Jose, CA 95134, USA
 Email: ruizhangece@gatech.edu

**Abstract:** The first 120Gbaud-based C-band self-homodyne 800Gb/s coherent links using low-latency FEC are experimentally demonstrated. A minimum coherent DSP is proposed to compensate fiber dispersion, phase mismatch between signal and local oscillator, and transceiver I-Q impairments. © 2022 The Author(s)

#### 1. Introduction

For intra-data center applications, a self-homodyne (SHD) coherent optical transceiver has a great potential to reduce the cost and power consumption of a conventional coherent transceiver. This is due to the fact that, by sending both the modulated signal and a copy of the transmitter laser (i.e., a remote local oscillator (LO)) to a receiver through two separate short optical fibers with similar lengths, the portion of digital signal processing (DSP) related to carrier frequency offset and carrier phase recovery can be removed. While at the same time, if a silicon-photonics-based adaptive polarization controller [1] can be built into a coherent receiver for the signal and/or remote LO, the portion of DSP related to polarization demultiplexing can also be removed [3-7]. Consequently, at a lower baud rate of 50~60+Gbaud [2,3] and 23 Gbaud [5], a "MIMO-free" coherent DSP was claimed possible, except that the in-/quadrature-(I-Q) phase rotation due to path-length mismatch between the signal and remote LO still needs to be corrected.

In this paper, assuming a low-latency forward error correction (FEC)-based bit-error-rate (BER) threshold, we experimentally demonstrate a single-carrier 800Gb/s SHD coherent link by using 120 Gbaud/DP-16QAM modulation. At this high baud rate, we found that a minimum receiver DSP based on a simple I-Q correction scheme is needed to compensate the combined effect of fiber dispersion, I-Q phase rotation, transmitter I-Q impairment, and receiver skew in combination with a finite analogue to digital convertor (ADC) resolution. The link was run at C-band to support the future high-capacity DWDM links required for artificial intelligence and machine learning [8,9].

## 2. Experimental Setup

Figure. 1 shows the experimental setup and DSP flow. At the transmitter side (Tx), four uncorrelated pulse amplitude modulation 4-level (PAM4) sequences were pre-equalized and loaded into a 120GS/s 70-GHz digital to analog

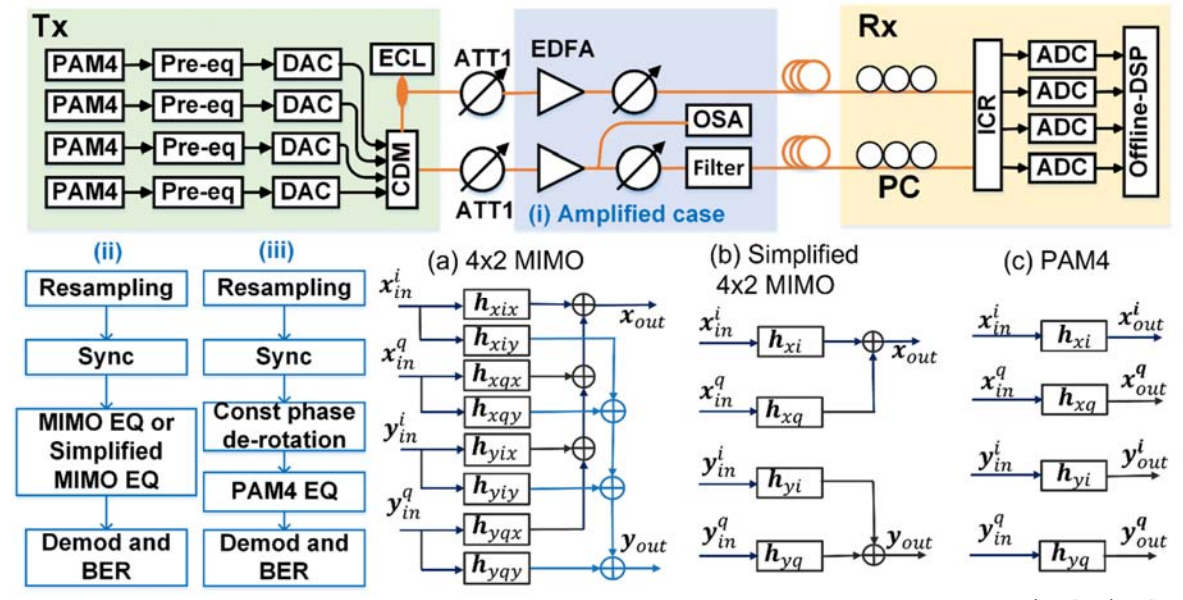


Fig 1. Experimental setup. (i) is used in amplified case. (ii) and (iii) are DSP block diagrams. (a) to (c): Equalizer principles.  $x_{in}^i, x_{in}^q, y_{in}^i, y_{in}^q, x_{out}^i$ ,  $x_{out}^q, y_{out}^i, y_{out}^q$  are real-valued PAM4 signal.  $x_{out}$  and  $y_{out}$  are complex 16QAM signal.

convertor (DAC) operating at 1 Sa/Symbol and passing through a coherent driver modulator (CDM), whose 3-dB bandwidth was 61 GHz. A 16.5 dBm external cavity laser is split into two paths using a 50:50 polarization maintaining (PM) coupler, which has a linewidth of 35 kHz and operates at a frequency around 193.1 THz. One path is used for Tx signal modulation and the other path for the remote LO through separate fibers to the coherent receiver (Rx). The optical power into CDM was 12.5 dBm and the remote LO launched into the transmission fiber was also 12.5 dBm. The output power from CDM is -9.5 dBm. Both amplified and un-amplified cases have been investigated experimentally. In the un-amplified case, we added a pair of attenuators (ATTs) in both the signal and the remote LO path, i.e., ATT1, to adjust the link losses of the two paths simultaneously. In the amplified case, we add one more pair of 21dBm Erbium-Doped Fiber Amplifiers (EDFAs) and ATTs in the link, as shown in Fig. 1 (i). The ATT1s emulate the loss of a 16-channel [9] DWDM multiplexer (MUX) and patch panel loss. Since the ATT1 loss changes the optical signal-to-noise ratio (OSNR), an optical spectrum analyzer (OSA) was added to monitor the OSNR after EDFA. Another pair of ATTs after EDFAs were used to emulate the link loss (and DWDM demultiplexer (DEMUX) loss for the signal path) and also adjust the signal and LO received optical power (ROP). A 1.5nm bandpass optical filter was placed before the receiver to remove the out-of-band amplified spontaneous emission noise. At Rx, a pair of polarization controllers (PCs) were used to recover the signal and remote LO state of polarizations (SOPs), respectively. The LO SOP is recovered to linear polarization by an automatic PC. The signal SOP is recovered by minimizing the X and Y polarization crosstalk, which can be achieved by monitoring the amplitude of low frequency (~ tens of KHz) dither tones inserted in each tributary [7] in both polarizations. An intradyne coherent receiver (ICR) with a bandwidth of 64GHz receives the signal and remote LO. The electrical signals were sampled by four 256 GS/s ADCs, and then processed by the offline DSP. We compare three DSP schemes as shown in Fig. 1 (ii) and (iii), which are 4×2 butterfly multiple-input multiple-output (MIMO) equalizer (EQ) at 2 Sa/symbol (as an ideal reference), simplified 4×2 MIMO EQ at 1.5 Sa/symbol (the proposed scheme), and PAM4 EQ at 1 Sa/symbol (the simplest DSP). After resampling and synchronization, the MIMO EQ or the simplified MIMO EQ was applied, and followed by signal demodulation and bit error rate (BER) counting. Since there is a slow time-varying I-Q phase rotation due to the path length mismatch between the signal and LO and/or ambient temperature and stress changes in the two fibers spools, a constant phase de-rotation (update period  $\approx 3.33 \times 10^{-5}$  s) was applied before PAM4 EQ. This is due to that PAM4 EQ treats I and Q independently and cannot deal with such a phase rotation. Fig. 1(a) to (c) show the three least-meansquare-based DSP structures. The 4×2 MIMO EQ considers both the I&Q crosstalk and X&Y crosstalk [10] while the simplified 4×2 MIMO EQ considers only the I&Q crosstalk. The complexity of our proposed simplified 4×2 MIMO

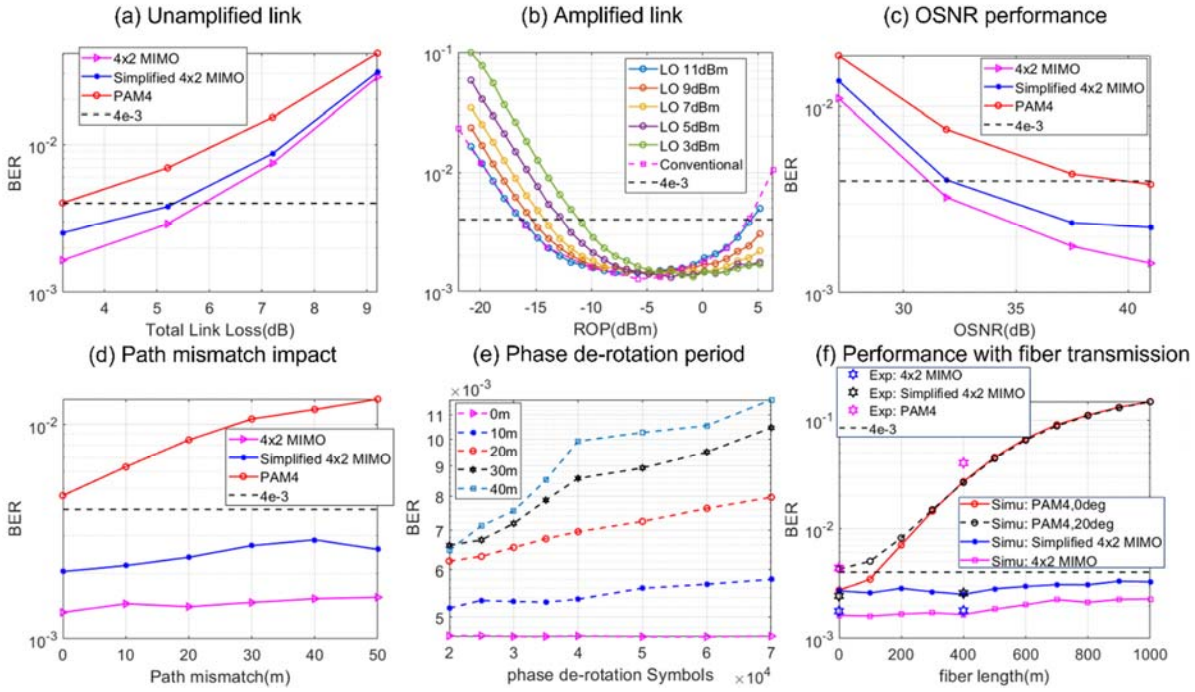


Fig 2. Experimental results. (a) Link budget of unamplified link. (b) Sensitivity performances with different LO power. (c) BER vs OSNR (LO = 3dBm, signal ROP=-0.5dBm). (d) BER vs path mismatch length (OSNR = 37.5dB, LO=3dBm, signal ROP = -0.5dBm) (e) BER vs Phase de-rotation period of PAM4 EQ (OSNR = 37.5dB, LO=3dBm, signal ROP = -0.5dBm). (f) BER versus fiber length (OSNR = 37.5dB, LO = 3dBm, star symbols are the experimental results). (a)-(c), (e), and (f) are with 0m path mismatch. The experimental results in (a)-(d) and (f) are after applying a constant phase de-rotation to the whole frame (114688 symbols).

is similar to an I&Q correction scheme [11], although the difference resides in that our algorithm minimizes the error of complex QAM symbols while [11] minimizes the error of each PAM symbol. Both the MIMO and simplified MIMO use 128 EQ taps. The PAM4 EQ with 129 taps processes the four PAM4 data independently, which can only remove the inter-symbol interference (ISI) due to bandwidth limitation.

#### 3. Experimental Results

Figure 2 shows the experimental results. Fig. 2(a)-(c), (e), and (f) are with 0m path mismatch. Fig. 2(a)-(d) and (f) show the results after applying a constant phase de-rotation to the whole frame (114688 symbols) in PAM4 EQ. First, we experimentally evaluate the link budget of the unamplified link in a back-to-back (BtB) without fiber dispersion case as shown in Fig. 2(a). The total link loss represents the loss of both the signal path and LO path. With respect to a low latency FEC BER threshold of  $4 \times 10^{-3}$ , PAM4 EQ can only support 3-dB link loss while  $4 \times 2$  MIMO and simplified 4×2 MIMO can support 5.9 dB and 5.2 dB, respectively. Next, we investigate the amplified links. Fig. 2(b) presents the BER performance versus ROP with different remote LO power into the ICR using 4×2 MIMO EQ. The optimal ROP for LO = 11 dBm is -5 dBm, whereas it changes to 0dBm for a reduced LO = 3 dBm. In the following experiments, we fix the received remote LO as 3 dBm and the signal ROP as -0.5 dBm to emulate a link loss of 5.5 dB (=21-10×log(16)-4-(-0.5)) between the EDFA and DEMUX, which considers that the 21dBm EDFA output power is shared by 16 DWDM channels, and a DEMUX loss of 4dB. The receiver sensitivity using a conventional LO and a 1:2 split ratio between LO and signal [12] was also presented for comparison, which shows a similar performance to the SHD case of LO = 11dBm. Next the scheme's OSNR tolerance was found by tuning the ATT1 to 0 dB, 5dB, 9dB, and 15dB, respectively. As shown in Fig.2(c), the PAM4 EQ gives the worst performance and exceeds the BER threshold when OSNR is smaller than 40 dB. We assume that the loss due to DWDM multiplexer and patch panel before EDFA is 5dB for both the signal and LO paths and obtain a fixed OSNR of 37.5 dB. Fig. 2(d) presents the BER performance as a function of path length mismatch between the signal and LO. The 4×2 MIMO and modified 4×2 MIMO show very small BER degradation when path mismatch varies from 0 to 50m, i.e., both are not sensitive to the phase variation due to path mismatch. This is because these two EQs minimize I and Q crosstalk, and therefore no additional phase de-rotation is needed. As for PAM4 EQ, a clear BER degradation can be observed for increased path length mismatch. Fig. 2(e) shows how the BER changes with different phase de-rotation update period (the phase rotation angle varies with time and therefore the corresponding digital phase de-rotation must be constantly updated) in terms of number of symbols when PAM EQ is used. The BER of 0m path length mismatch is independent of the phase de-rotation update period while for 10 to 50m mismatch the BER increases when the phase de-rotation update period increases. Fig. 2(f) shows the simulation (in solid lines) and experimental results (in star symbols) of BER versus fiber transmission length, and they match well. When the fiber length is 0m, the PAM4 EQ can have the same BER performance as that of the simplified MIMO, but two factors make PAM4 EQ's BER further degrade: (1) when the I-Q rotation angle is nonzero (e.g., 20-degree in Fig. 2(f)), and (2) fiber chromatic dispersion. Factor (1) is caused by the finite ADC resolution (e.g., ENOB=5.5 in the simulation) which forbids a precise de-rotation angle of the I-Q constellation. We have verified by simulation that PAM4 EQ causes significant BER degradation when both receiver skew and I-Q phase rotation exist, while a higher ADC resolution (e.g., ENOB=13) can improve the performance. Factor (2), which can be modeled as a complex finite impulse response (FIR) filter in time domain [13], causes frequency-dependent I-Q mixing and ISI. As shown in Fig.2(f), modified 4×2 MIMO EQ can easily exhibit a BER lower than the  $4 \times 10^{-3}$  threshold up to 1km of standard single-mode fiber, while PAM4-based DSP cannot achieve a BER lower than the threshold considering a randomly rotated received I-Q constellation.

#### 4. Conclusions

Through experiments and simulations, we have demonstrated a 120-Gbaud DP-16QAM self-homodyne coherent system (a net data rate of >800Gb/s) with link budgets of 4.5 dB (for amplified 16 DWDM channels, which can be extended to 6.5dB if 23dBm EDFAs were used) and 5.2 dB (unamplified single-channel case) via a low-latency FEC and a simplified 4×2 MIMO DSP algorithm, which can correct (a) fiber chromatic dispersion for at least 1km, (b) the random I-Q rotation angle caused by the length mismatch between the signal and remote LO paths, and (c) the transceiver I&Q impairments. The amplified DWDM can greatly enhance the link capacity in comparing to the unamplified case, thus C-band DWDM SHD transceiver is very promising for future intra-data center applications.

### 5. References

- [1] X. Wang, et al., paper Th1A.33, OFC 2021.
- [2] L. Wang, et al., paper Th3C2-PD1.5, ECOC 2021.
- [3] M. Morsy-Osman, et al., Opt. Express 26, pp. 8890, 2018.
- [4] T. Gui, et al., paper Th4C.3, OFC 2020.
- $[5]\ L.\ Wang,\ et\ al.,\ paper\ M5G.3.,\ OFC,\ 2021.$
- [6] T. Gui, et al., paper T5A.5, OECC 2021.
- [7] J. K. Perin, et al., J. Light. Technol 35, pp. 4650, 2017.
- [8] K. Schmidtke et al., paper W1E.5, OFC 2021.
- [9] www.oiforum.com/technical-work/hot-topics/800g-coherent
- [10] R. Rios-Müller, et al, ECOC 2014.
- [11] C. R. S. Fludger and T. Kupfer, ECOC 2016, pp. 1-3.
- [12] Y.-W. Chen, et al., paper T5A.9, OECC 2021.
- [13] K.-S. Kim, et al., J. Opt. Soc. Korea 12, pp. 249, 2008.